

# COMPARING TWO TYPES OF VHF LOW-NOISE FREQUENCY SOURCES FOR MICROWAVE AND HIGHER FREQUENCY SYNTHESIS

Takeo Oita\*, Fumio Asamura, and Katsuaki Sakamoto  
 Nihon Dempa Kogyo Co., Ltd., Japan  
 E-mail: oita@ndk.com

## Abstract

*The Butler and modified Butler-type crystal oscillator circuits have been selected as the candidates to develop low-noise 100 MHz VHF crystal oscillators using SC-cut crystals. A low-noise buffer amplifier with a matching circuit to the 50-ohm output load is commonly used for these two design models. Evaluations of the phase noise performance have been achieved by comparing predicted performance and experimental results for the phase noise performance of each of the two types. The Butler-type phase noise is shown to be less than  $-162$  dBc/Hz in actual results compared with the predicted value of  $-170$  dBc/Hz at a 10 kHz Fourier frequency. The modified Butler-type shows less than  $-171$  dBc/Hz in actual results, compared with the predicted value of  $-178$  dBc/Hz at the same Fourier frequency.*

## 1. INTRODUCTION

Low-noise higher frequency reference sources have been used for precision time and frequency measurement equipment and Doppler radar systems. Additionally, sophisticated broadband telecom systems, such as MIMO systems, and point-to-point microwave telecom network systems have been becoming popular. The lower noise of the microwave local oscillators have been becoming more and more important. The higher frequency low-noise reference sources of PLL systems are preferred because of their dividing ratio's reduction.

Figure 1 shows the functional schematic diagrams of the crystal-controlled oscillator.

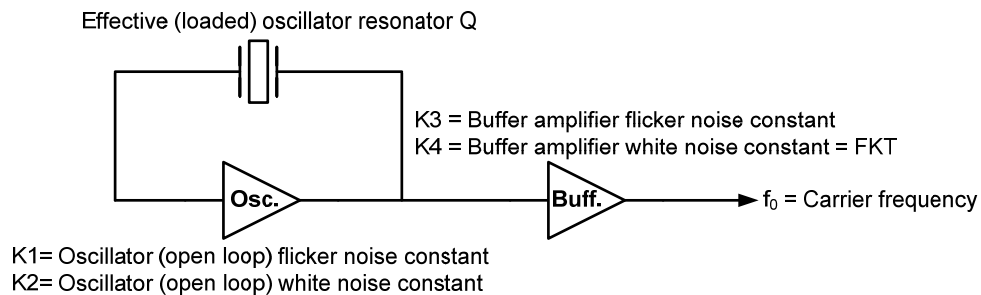


Figure 1. Functional schematic diagrams of the crystal controlled oscillator.

The spectral density of the phase fluctuations of the output signal of the circuit in Figure 1 can be expressed as formula (1) [1,2]:

$$S_{\delta\phi}(f) = 2 \left[ \left( \frac{K1}{f} + K2 \right) \left( \frac{1}{d\phi/df} \right)^2 \left( \frac{1}{f} \right)^2 + \frac{K3}{f} + K4 \right] \quad (1)$$

The SSB phase noise power ratio is defined as formula (2) [1,2]:

$$L(f) = 10 \log[ S_{\delta\phi}(f) / 2 ]. \quad (2)$$

On the other hand, to discuss the short-term stability in the field of the time domain, a translation to the Allan variance from the frequency domain to the time domain can be expressed as formula (3) [3]:

$$\sigma^2_y(\tau) = 2 \int_0^{\infty} S_{\delta\phi}(f) \left[ \frac{\sin^4(\pi f \tau)}{(\pi f_0 \tau)^2} \right] df \quad (3)$$

Considering the above, the following subjects have been studied carefully:

- The SC-cut crystal resonator is preferred for application to the 30 dB/decade region
- The nonlinear effects of the oscillator's open loop, and buffer amplifiers as the active device should be considered for application to the 1/f noise, 10 dB/decade region
- The oscillator output signal level should be also considered, comparing the white noise of the oscillator open-loop active device and the buffer amplifier's own white noise.

Table 1 shows the equivalent constant value of the 5<sup>th</sup> overtone SC-cut crystal that was used for the predictions and experiments.

Table 1. Equivalent circuit constant of 5<sup>th</sup> overtone SC-cut crystal.

	C-Mode	B-Mode
F <sub>0</sub> [MHz]	100.000045	109.311544
Q	133,636	482,193
CI [ohms]	114.67	67.30
C <sub>0</sub> [pF]	3.733	-----
C <sub>1</sub> [fF]	0.104	0.045
C <sub>0</sub> /C <sub>1</sub>	35924.8	-----
L1 [mH]	24.389	47.248
zTc [degC]	84.4	-----

## 2. BUTLER-TYPE OSCILLATOR

Figure 2 shows the functional schematic diagram of the Butler-type 5<sup>th</sup> overtone SC-cut crystal-controlled oscillator.

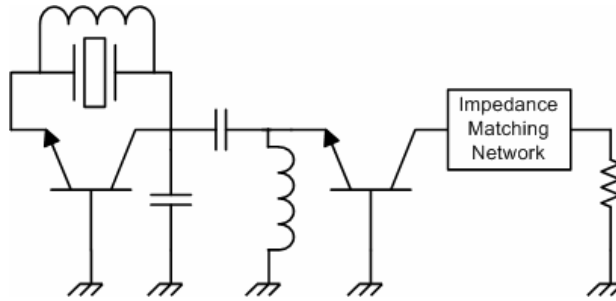


Figure 2. Functional schematic diagrams of the Butler-type oscillator (self-limiting).

The base of both of the BJTs of the oscillator loop and the buffer amplifier are connected to the ground; it can be expected to have the low noise of a low-noise oscillator. The resonance frequency of the LC resonator in the oscillator loop can keep the stable excitation of the C-mode of the SC-cut crystal to avoid the B-mode excitation. Figure 3 shows the predicted gain/phase locus chart of the oscillator loop. The stable C-mode excitation would be fully expected, and the loop gain at the B-mode frequency will be fully suppressed. The oscillator signal is taken from the collector of the BJT of the oscillator loop, and led to the emitter of the buffer amplifier, which has low input impedance, so impedance matching between the oscillator loop and the buffer amplifier should be considered carefully.

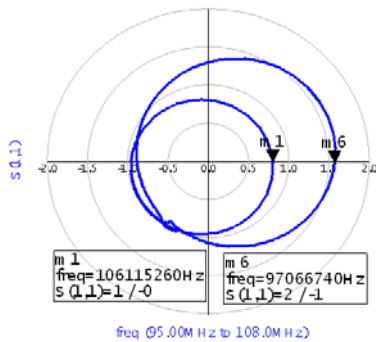


Figure 3. Gain/phase locus.

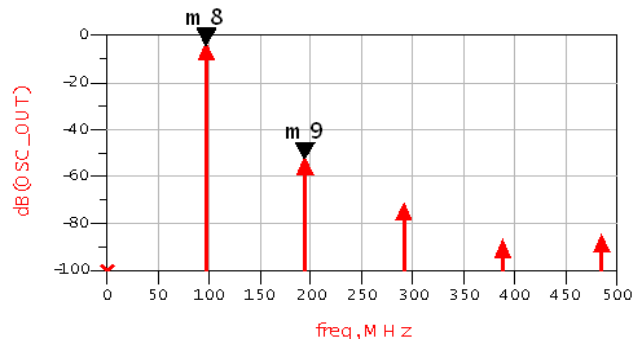


Figure 4. Predicted output signal spectrum.

Figure 4 shows the predicted output signal spectrum. The impedance-matching network is very important in order to suppress the harmonics which sometimes cause malignant problems in the sub-micro and microwave receiver's front-end low-noise amplifier or mixer, as unwanted signals from the local oscillator. The second harmonics would be suppressed -50 dB from the carrier frequency.

Figure 5 shows the predicted phase noise performance at 85 deg C.

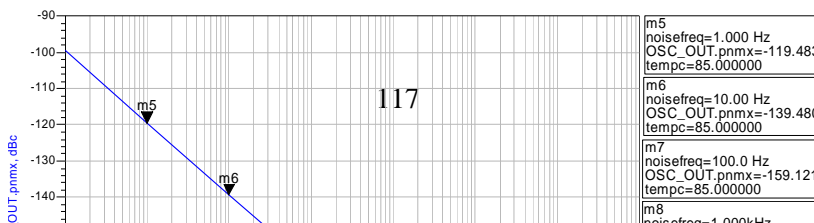


Figure 5. Predicted phase noise performance at 85 deg C (Butler-type)

## 2. MODIFIED BUTLER-TYPE OSCILLATOR

Figure 6 shows the functional schematic diagram of the Modified Butler-type 5<sup>th</sup> overtone SC-cut crystal-controlled oscillator.

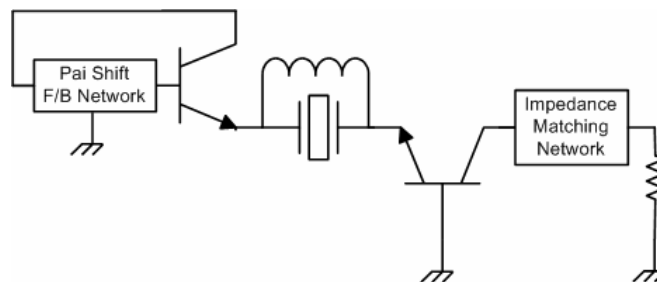


Figure 6. Functional schematic diagrams of the Modified Butler-type oscillator (self-limiting).

The sustain stage of the oscillator loop consists of a 180-degree feedback network, and the crystal resonator is connected in series to the emitter of the oscillator-loop active device. The oscillation signal from the sustain stage is fed through the crystal resonator and its output signal drives the buffer amplifier, which has low input impedance. The loss of the feedback network and the phase-shifting performance of the sustain stage should be considered carefully so that the particular stable C-mode excitation can keep the B-mode suppressed. Figure 7 shows the oscillator gain/phase locus chart of the Modified Butler-type.

It is easy to get the high oscillator loop gain compared with the Butler-type, but the optimization of the oscillator loop depends upon the trade-off between the gain at C/B-mode frequency, the loss of feedback network of the sustain stage, and the oscillation level for the higher C/N. Figure 8 shows the predicted output signal spectrum. The second harmonics would be suppressed about -35 dB from the carrier. Since a high gain of the sustain stage is easy to get, the optimization of the particular level to avoid the nonlinear effect of both of the sustaining amplifier and buffer amplifier should be considered carefully.

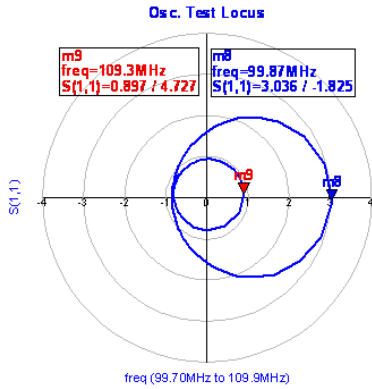


Figure 7. Gain/phase locus.

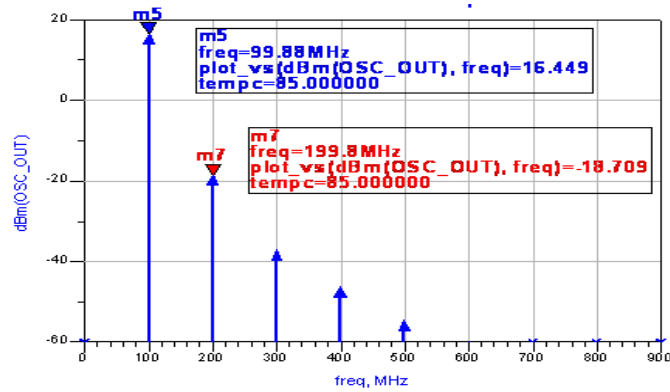


Figure 8. Predicted output signal spectrum.

Figure 9 shows the predicted phase noise performance at 85 deg C.

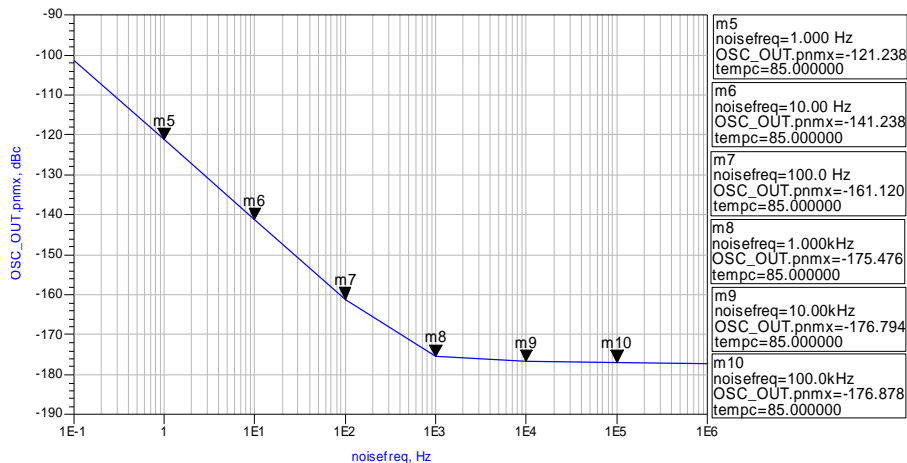


Figure 9. Predicted phase noise performance at 85 deg C (Modified Butler-type).

### 3. OCXO DESIGN AND PERFORMANCE

The temperature coefficient of the oscillator circuit without the quartz resonator in the OCXO package should be also considered carefully so as to be a stable reference oscillator [4]. Each component has its own temperature coefficient and is placed at some position on the printed circuit board where the temperature changes by the ambient temperature variation. The comprehensive temperature coefficient of the oscillator circuit depends upon such physical conditions according to its construction. The temperature coefficient has been decreased less than -9 ppb/deg C by using thermal analytic results and temperature compensation methods. Figure 10 shows the simplified functional block diagram for the experiments. Both the power and the thermal regulators are also designed to avoid the noise effects to

the oscillator circuit. The thermal sources are set closer to the quartz crystal, and the thermal sensor is set between the thermal sources and the quartz resonator. The 50 ohms pad is placed before the output to reduce the effect of the reflected signal from the load to the oscillator.

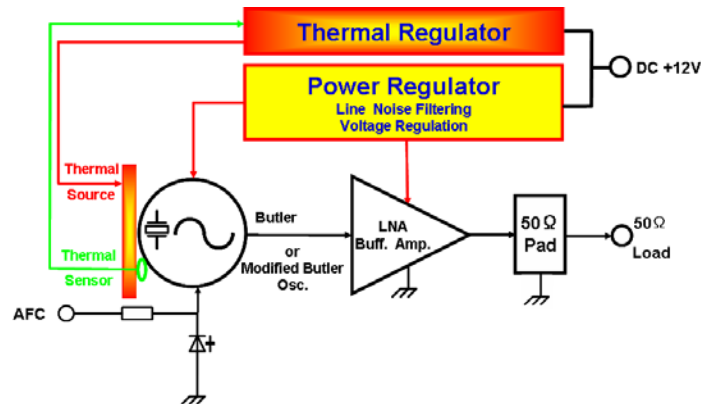


Figure 10. Simplified functional block diagram of the OCXO.

Figure 11 shows the inside of the OCXO which is used for the trial experiments. The HC-43/U crystal unit is set under the PCB without the oven mass to reduce the total power consumption. Figure 12 shows the resistance-welded hermetic-sealed package, whose size is 25.4x25.4x12.7 mm, and lead-free designed.

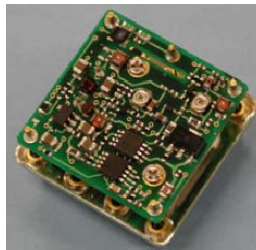


Figure 11. Inside of the OCXO.



Figure 12. Finished package.

Figure 13 shows some sample graphs of the frequency temperature stability performance, which are after some temperature compensation adjustment, such as oven temperature to zero temperature coefficient for both types of crystal oscillators. These perform sufficiently within  $\pm 20$  parts per billion over the temperature range from -20 deg C to +70 deg C. Figure 14 shows the typical performance of the long-term frequency stability, adding the fitted line. It is expected to be less than +400 parts per billion over 3 years.

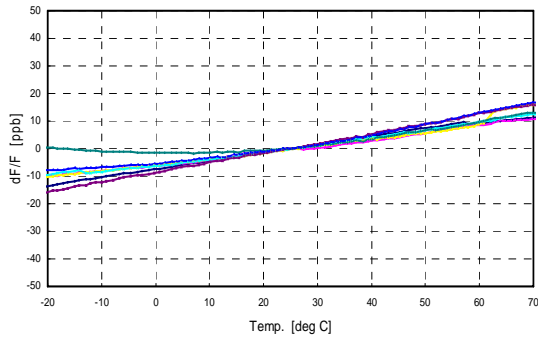


Figure 13. Freq.-temp. performances.

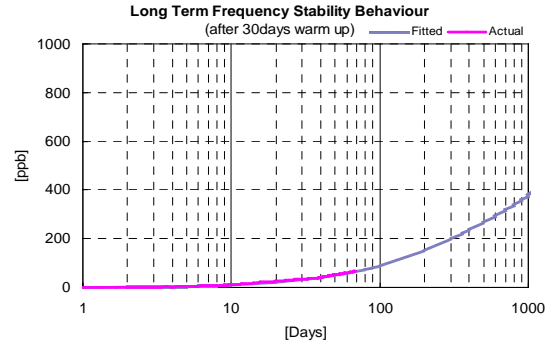


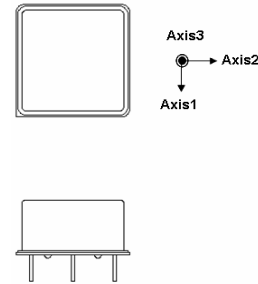
Figure 14. Frequency ageing performance.

Table 2 shows the acceleration sensitivity (2-g tip-over) test results.

Table 2. Acceleration sensitivity (2-g tip-over test).

[Unit in ppb]

Osc. No.	Axis1	Axis2	Axis3	AxisNet
A	2.50	0.40	0.80	2.66
B	-2.60	0.45	-0.35	2.66
C	-2.70	0.60	-1.10	2.98



#### 4. PHASE NOISE AND SHORT-TERM STABILITY COMPARISON

Figure 15 shows the test results of the phase noise performance of the Butler-type oscillator. Figure 16 shows the Modified Butler-type performance. Table 3 shows the summary of the phase noise comparison of the two types of the oscillator phase noise performance.

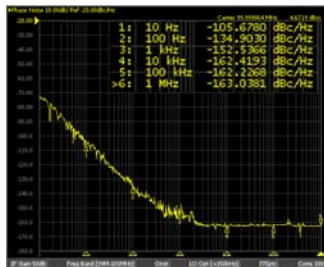


Figure 15. Butler

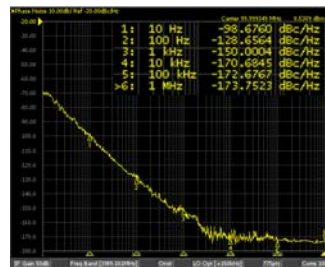


Figure 16. Modified Butler

Table 3. Phase noise comparison.

Item	Butler Type		Modified Butler Type	
	Experiments	Predictions	Experiments	Predictions
Offset				
@10Hz	-105.7dBc/Hz	-139.5dBc/Hz	-98.7dBc/Hz	-121.2dBc/Hz
@100Hz	-134.9dBc/Hz	-159.1dBc/Hz	-128.7dBc/Hz	-161.1dBc/Hz
@1kHz	-152.5dBc/Hz	-169.3dBc/Hz	-150.0dBc/Hz	-175.5dBc/Hz
@10kHz	-162.4dBc/Hz	-169.7dBc/Hz	-170.9dBc/Hz	-176.8dBc/Hz
@100kHz	-162.2dBc/Hz	-169.7dBc/Hz	-172.7dBc/Hz	-176.8dBc/Hz
>@1MHz	-163.0dBc/Hz	-170.2dBc/Hz	-173.8dBc/Hz	-177.0dBc/Hz

Since there is not much commercialized equipment for high frequency and precision time interval measurement in the VHF range and at a 10 ms averaging time, we used an “Anritsu, SD5M02A” to measure the Allan deviation for each type of oscillator. Figure 17 shows the comparison of the

short-term stability test results of both two types of oscillators. The “-160 dBc/Hz type” means the Butler-type, and the “-170 dBc/Hz type” means the Modified Butler-type. The fluctuation of the Modified Butler-type in the range of 30 ms to 80 ms is considered to be the noise effect from the 50 Hz electric line. It is observed to be less than  $10^{-11}$  at a 100 ms averaging time for both oscillator types.

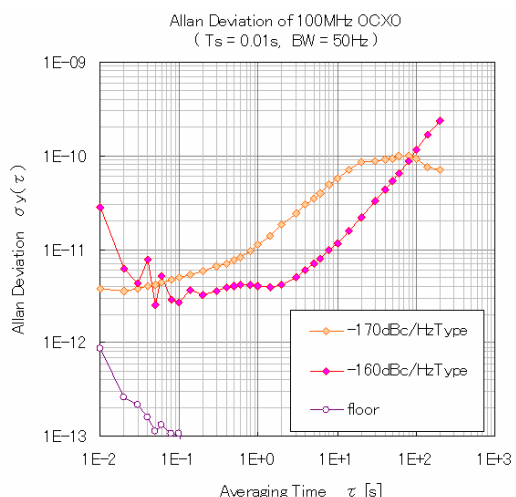


Figure 17. Allan deviation comparison.

## 5. CONCLUSIONS

We have achieved two types of VHF-range low-noise oscillators: one is the Butler-type and the other is the Modified Butler-type. Both of these types of oscillator have good performance of low phase noise, which is suitable as VHF frequency reference sources for microwave and higher frequency synthesis and some special applications. The second harmonics (not shown in this paper) has been suppressed to less than -50 dBc, which gives the optimum performance for the local oscillator synthesizer for the telecom base stations and wideband receiver applications. The Butler-type OCXO has been announced already as the 9325D type, whose output frequency covers 80 MHz to 135 MHz, and the other type will be increasingly unveiled. Since we have many experiences with the SC-cut crystals covering from HF to VHF in frequency range, the core technology of these low-noise VHF OCXOs will be applied for our low-noise microwave frequency synthesizer and UHF low noise reference signal source, along with improving the size reduction for the lower power, and the acceleration sensitivity with the improved quartz crystal package.

## REFERENCES

- [1] D. B. Leeson, 1966, “A Simple Model of Feedback Oscillator Noise Spectrum,” **Proceedings of the IEEE**, **54**, 329-330.
- [2] M. M. Driscoll, 1986, “Low Noise, VHF Crystal-Controlled Oscillator Utilizing Dual, SC-Cut Resonators,” **IEEE Transactions on UFFC**, **UFFC-33**, 698-.
- [3] D. Allan, 2006, “Time Domain,” in NIST 2006 Time and Frequency Metrology Seminar, chap. 2.
- [4] R. K. Karlquist, L. S. Cutler, E. M. Ingman, J. L. Johnson, and T. Parisek, 1997, “A Low-Profile High-Performance Crystal Oscillator for Timekeeping Applications,” in Proceedings of the 1997 IEEE International Frequency Control Symposium, 28-30 May 1997, Orlando, Florida, USA (IEEE 97CH36016), pp. 873-884.